Advanced Optimization of an Isoflux Reflectarray

Andrea Guarriello, Renaud Loison, Daniele Bresciani, Herve Legay, George Goussetis

Advanced Optimization of an Isoflux Reflectarray

Andrea Guarriello* †, Renaud Loison* , Daniele Bresciani‡, Hervé Legay‡, George Goussetis†
*IETR, National Institute of Applied Sciences, Rennes, France, Andrea.Guarriello@insa-rennes.fr
†Institute of Sensors, Signals and Systems, Heriot-Watt University, Edinburgh, United Kingdom
‡Direction of Research, Thales Alenia Space, France

***Abstract*—This paper presents a method for the optimization of the cross-polar component of a circularly polarized isoflux reflectarray (RA) for payload data handling and transmission. The advanced optimization technique consists of an efficient lookup table parametrization employed in a direct radiation pattern optimization of the RA through minimax algorithms. The lookup table parametrization is employed in a spline projection of the RA cells distribution. The spline coefficients are modulated to achieve a sectorial bilateral isoflux radiation pattern with cross-polar discrimination superior to 15 dB. The RA optimization is performed by considering cells local periodicity that is naturally ensured by the spline projection of the RA layout.**

***Index Terms*—Reflectarray optimization, isoflux pattern, minimax optimization, spline surfaces projection.**

I. Introduction

Payload data handling and transmission (PDHT) for low earth orbit satellites demand antennas able to transmit at the ground station in a time window that is limited to the visibility time of the satellite passage, typically when the satellite is at least at 5° of elevation from the ground station (GS). To maximize the link-time during the GS passage, isoflux-shaped beams are sought to compensate for the path loss in a specified wide angular range. LEO spacecraft antennas employed to produce gain isoflux patterns in circular polarization are mainly helix antennas [1], [2] and choke ring horns [3], [4], [5], in recent years lightweight planar antennas, such as meta-surfaces [6], [7], [8] and reflectarrays [9], [10], are topic of research, with particular emphasis on applications such as high-gain global coverage in satellites mega-constellations [11].

Recent PDHT systems present stringent performances, such as working in double circular polarization with high levels of cross-polar discrimination (XPD). Obtaining a radiated field polarization purity at high radiation angles is a challenging task for aperture antennas. In [3], [4] and [8] it has been shown how the amplitude control of the aperture field is a key point of the design process of an aperture field able to produce an isoflux beam with high XPD over a very large angular region.

Reflectarray (RA) antennas are an attractive solution for small satellites application in virtue of their features linked to mass, cost, and foldability. RAs with the requirements of an isoflux beam for LEO satellites with high XPD is a quite challenging case since passive RA antennas present some limitations in the control of the aperture field amplitude since it strongly depends on the incident field amplitude distribution [12]. Previous works on RAs radiating circular polarization isoflux patterns can be found in [9], [10], where also the issue of the cross-polar reduction has been addressed. The novelty of our work, compared to the latest ones, is that the angular aperture of the beam is broader, allowing the application of such antenna in LEO satellites.

To this extent, this paper focuses on the optimization of the circular polarization purity of planar high-gain broad-beam RA by applying an original approach exploiting the rebirth properties of Phoenix cells [13], [14]. The application objective is to conceive a physically small RA (diameter of 300 mm) radiating a sectorial isoflux beam spanning between -60° and 60° and working in Ka-band ($f_0 = 26.25$ GHz). The paper is structured as follows: the reference isoflux mask is computed in section II and section III presents the optimization process methodology applied to an isoflux RA composed of Phoenix cells. Finally, section IV gives some conclusions.

II. Isoflux mask construction

The sectorial isoflux coverage specifications are directly linked to the spacecraft/ground distance when the satellite is visible from the GS. We assume that the satellite is visible when it is at least at 5° of elevation. The link between the path losses and the distance spacecraft/GS over an angular range can be expressed by the relation

$$PL(\theta) = \frac{(h+R_e)\cos\theta - \sqrt{\left[(h+R_e)\cos\theta\right]^2 - (h^2+2hR_e)}}{h} \tag{1}$$

where h is the orbit altitude and R_e is the Earth radius. In this paper, the reference orbit is a circular orbit with an altitude of 700 km and the angular range for which the satellite is visible from the GS is $[-60^\circ, 60^\circ]$. The isoflux mask concerns the plane $\phi = 90^\circ$ while, in the orthogonal plane $\phi = 0^\circ$, the beam is directive.

III. Avdanced optimization methodology

The general RA design methodology is articulated in several steps, each one implying comprehensive physical and mathematical models.

A. RA architecture

The definition of the RA architecture is the first step of the design process. In this work, a reference conventional reflector, whose complete radiation features are analyzed, or a target radiation pattern (or far-field mask) is supplied, allowing to establish the RA target performances or to compute a first guess solution. The feeding system is known as well. From

the performance/system specifications, the RA architecture is consequently chosen. Once all of these input data are defined, it is possible to derive the target aperture field, the incident field, and incidence angles distribution on the RA surface. Therefore, the RA main design parameters are chosen or imposed in this stage (antenna geometry and size, operational frequency, lattice size, etc.).

The RA surveyed comprises a single layer monolithic panel fed by a conventional onset horn working in the frequency band $f = [25.5; 27.00]$ GHz with a center frequency of 26.25 GHz (Figure 1). The RA is circular with a diameter fixed to 300 mm, corresponding to roughly 26.3λ (λ the free-space wavelength at the center frequency). In this work, the bandwidth issue is not addressed, so only the central frequency is considered in the following.

The horn illuminates the RA panel with an onset-centered configuration with $f/D = 0.52$ in right and left hand circular polarization (*RHCP* and *LHCP*) with a taper of $11.5\,dB$ on the RA edge. The RA parameters are summarized in Table I referring to the coordinate system and definitions shown in Figure 1.

TABLE I: RA features

Operational frequency	$f = 26.25$ GHz
RA geometry	circular
Dimensions	$D_x = D_y = 26.3\lambda$
Unit cell lattice	$p_x = p_y = 0.33\lambda$
Number of cells	4899
Substrate thickness	$t = 1.524$ mm
Substrate	RO4003C
Focal distance	$F = 156.7$ mm
Feed offset angle	$\theta^f = 0°$

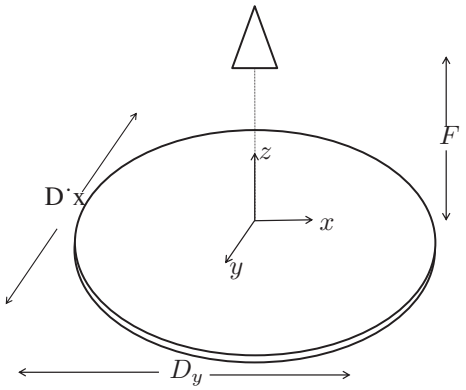

Fig. 1: RA antenna geometry

B. Elementary cells look-up table construction

The elementary cell geometries are chosen according to their scattering properties. Once the geometries of the elementary cells are defined, their reflective properties as a function of the degrees of freedom (geometrical parameter of the cells) are characterized [15], a lookup table is built. The lookup table contains all the elementary cell geometries and their scattering properties at different incidence angles and frequencies (defined in the RA analysis step). Therefore, the lookup table is conveniently parameterized and mapped against suitable design parameters and interpolated via continuous cubic functions.

In this work, the first and second-order inductive Phoenix cells are selected (Figure 2). The chosen cycle avoids sharp geometrical transitions for adjacent cells. The lookup table is subsequently linearly parametrized against an auxiliary periodic variable ξ.

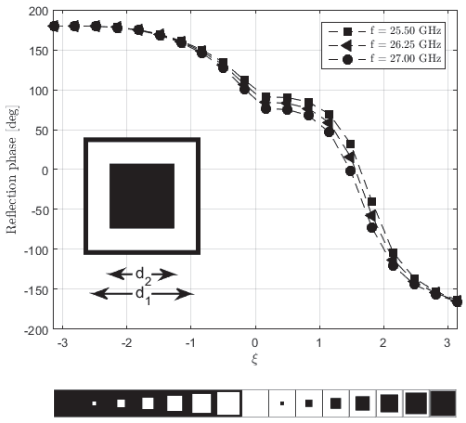

Fig. 2: Phase of the scattering coefficient of a square loop/slot combination element in a periodic environment as function of the periodic parameter ξ describing the geometry. In the inset the relevant parameters defining the cell's geometry.

To extend the geometric degrees of freedom of the cells while preserving the lookup table regularity and smoothness, the square Phoenix cells are distorted into rectangles. This allows to control the impinging wave delay and compensate for depolarization [16]. The parametrization of the new lookup table leads to a cylindrical mapping (Figure 3) of the geometries stored in the look-up table, in which the ξ variable represents the index of the periodic cycle, while h the cells distortion index bounded between $[-1, 1]$. This representation is particularly convenient in the advanced RA optimization process. Indeed it provides a powerful tool for selecting adjacent cells with similar geometrical parameters by selecting the cylindrical coordinates (ξ, h) in a continuous domain. A local cubic interpolation of the scattering properties against the index of the cell is performed to have fast access to the lookup table during the optimization process.

C. RA layout synthesis and optimization

The RA quasi-periodic cells distribution, i.e., the RA layout, is built in this stage. After constructing a first guess layout composed of the cells available in the lookup tables previously defined, the RA is optimized to comply with specific performances.

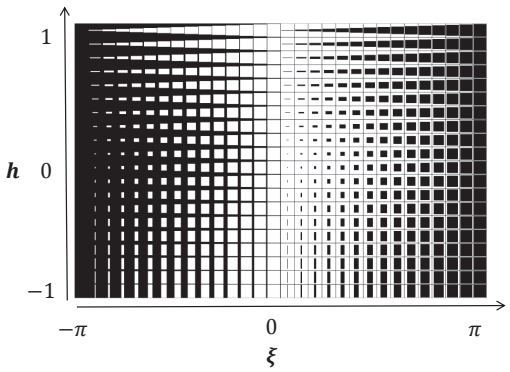

Fig. 3: Lookup table cylindrical mapping representation, open cylinder view.

The optimization consists in formulating a minimax problem by considering a cost function defined as the amplitude error of the RA radiated far-field against a specified mask. The cost function is minimized by directly adjusting the geometric parameters of the cells composing the RA layout at a global level. The optimization variables state vector is hence defined as a surface distribution of the index of the cell composing the lookup table previously parametrized.

The parametric surface distribution on the RA is described through continuous tensorial spline representation. The global representation of the RA layout through parametric splines surfaces offers the advantage of a continuous distribution of cells geometries over the RA layout. Thus the representation of the RA layout as continuous and smooth spline surfaces naturally avoids sharp geometric transitions on the RA surface. The quasi-periodicity constraint is, therefore, naturally respected. Moreover, this representation implies a reduction of the optimization problem variables dimensions, reducing the computational effort of the optimization. Indeed, the parametric spline surface is described on a very limited set of knots compared to the actual number of cells geometries composing the layout. The number of knots is directly related to the dimensions of the spline coefficients that are the optimization variables state vector.

The direct optimization is performed in three steps. The first step consists in obtaining a first guess solution. The preliminary layout design is performed with a classical phase only (PO) synthesis. A preliminary targeted phase law is derived by considering a hyperbolic paraboloid-shaped metallic reflector previously designed, but whose radiation patterns cannot comply with the mask. This is due principally to spillover and incident field tapering issues of the highly shaped reflector. The layout obtained is used as a first guess solution for the subsequent direct optimization of the Co-polarization levels, which represent the second step. In the first two steps, the uni-dimensional lookup table of figure 2 is employed. The results of the direct Co-polarization are shown in figure 4. We can see that the RA radiation patterns can withstand the mask levels. The cross-polar levels, on the contrary, do not allow the double polarization mode, since the cross-polar levels are too high for angles beyond $\pm 40°$.

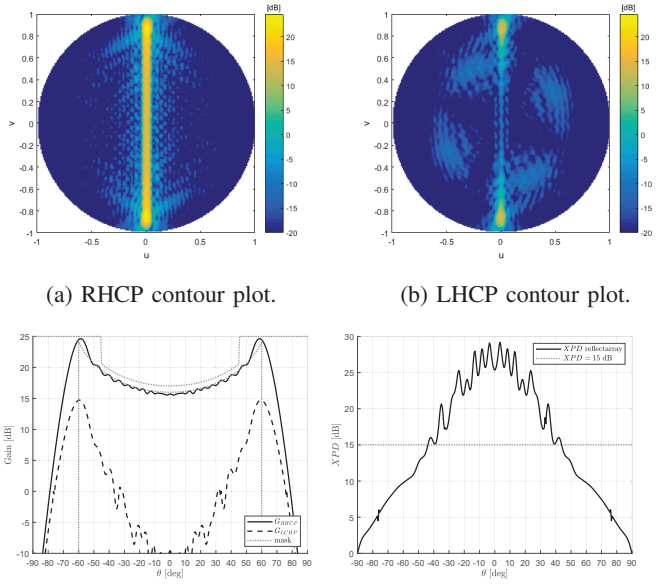

(a) RHCP contour plot.

(b) LHCP contour plot.

(c) Radiation in cut $\phi = 90°$.

(d) XPD in cut $\phi = 90°$.

Fig. 4: Co-polarization optimized RA radiation pattern.

The high levels of cross-polar at high radiation angles are caused by the lack of an amplitude control of the reflected field from passive RA cells[12]. Even if a passive RA element cannot efficiently control the amplitude levels of the aperture field, a direct optimization in which the RA square patches and slots are deformed into rectangles can allow phase or amplitude compensation that a global level can enhance the XPD levels (where $XPD = \frac{G_{RHCP}}{G_{LHCP}}$).

This time the objective is to minimize the maximum error between the radiation pattern and the prescribed mask by varying the (ξ, h) parameters (described in Figure 3) on the RA surface. The initial condition is the single polarization design, for which the h parameter distribution is null everywhere since square cells have been adopted. The optimization is performed at the center frequency $f_0 = 26.25$ GHz. Figure 5 shows the optimized layout.

The optimized RA patterns now comply with the XPD requirements preserving the co-polar isoflux envelope, but it presents some gain losses (Figure 6). By looking at the contour plots of Figures 6a, 6b, we can notice that part of the energy lost on the main cut has been distributed on the cross-polar component and some secondary lobes appear on the orthogonal cut, as it can be noticed from figure 6a.

IV. Conclusions

This paper presented the advanced optimization of a bilateral sectorial isolfux RA for small satellites PDHT. Substantial improvements on the XPD levels can be achieved through a direct optimization technique implying deformed Phoenix cells, at the cost of degradation on the co-polarization levels.

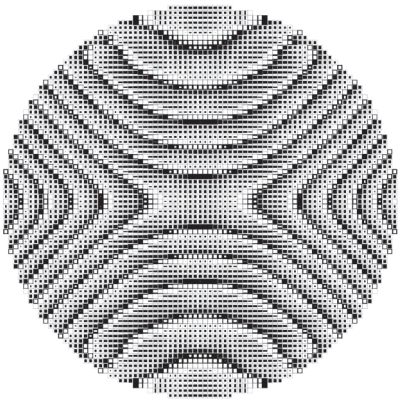

Fig. 5: Optimized RA layout

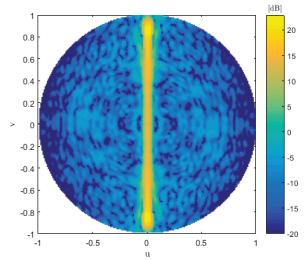

(a) RHCP contour plot.

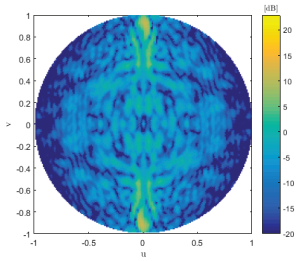

(b) LHCP contour plot.

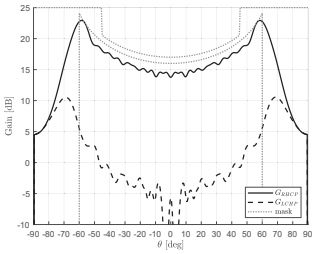

(c) Radiation in cut $\phi = 90°$.

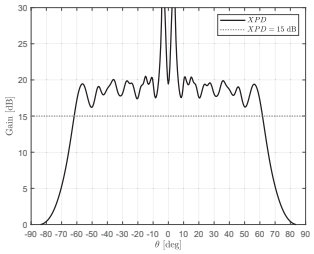

(d) XPD in cut $\phi = 90°$.

Fig. 6: Crosspolar optimized RA radiation pattern.

The presented methodology is sought to overcome the limitations on amplitude modulation imposed on passive RA cells. This study confirmed the impact of the limitations of passive RA cells to modulate the aperture field amplitude, which is necessary to achieve high XPD at highly tilted radiating angles. Future works would include shaping the incident field components coming from the primary source. Enabling feed amplitude shaping would allow approaching the target aperture field components amplitude.

ACKNOWLEDGMENT

This work was supported by the European Commission under the H2020 project REVOLVE (MSCA-ITN-2016-722840). The authors would like to thank Kevin Elis (CNES) for supplying a reference metallic reflector, the feed, and the design constraints.

REFERENCES

[1] R. Manrique, G. Le Fur, N. Adnet, L. Duchesne, J. M. Baracco, and K. Elis. Telemetry x-band antenna payload for nano-satellites. In *2017 11th European Conference on Antennas and Propagation (EUCAP)*, pages 549–552, 2017.

[2] M. Taherkhani, J. Tayebpour, S. Radiom, and H. Aliakbarian. Circularly polarised wideband quadrifilar helix antenna with ultra-wide beamwidth isoflux pattern for a s-band satellite ground station. *IET Microwaves, Antennas Propagation*, 13(10):1699–1704, 2019.

[3] E. Arnaud, J. Dugenet, K. Elis, A. Girardot, D. Guihard, C. Menudier, T. Monediere, F. Roziere, and M. Thevenot. Compact isoflux x-band payload telemetry antenna with simultaneous dual circular polarization for leo satellite applications. *IEEE Antennas and Wireless Propagation Letters*, 19(10):1679–1683, 2020.

[4] J. Fouany, M. Thevenot, E. Arnaud, F. Torres, C. Menudier, T. Monediere, and K. Elis. New concept of telemetry x-band circularly polarized antenna payload for cubesat. *IEEE Antennas and Wireless Propagation Letters*, 16:2987–2991, 2017.

[5] R. Ravanelli, C. Iannicelli, N. Baldecchi, and F. Franchini. Multi-objective optimization of an isoflux antenna for leo satellite down-handling link. In *18-th International Conference on Microwaves, Radar and Wireless Communications*, pages 1–4, 2010.

[6] G. Minatti, S. Maci, P. De Vita, A. Freni, and M. Sabbadini. A circularly-polarized isoflux antenna based on anisotropic metasurface. *IEEE Transactions on Antennas and Propagation*, 60(11):4998–5009, 2012.

[7] G. Minatti, M. Faenzi, E. Martini, F. Caminita, P. De Vita, D. González-Ovejero, M. Sabbadini, and S. Maci. Modulated metasurface antennas for space: Synthesis, analysis and realizations. *IEEE Transactions on Antennas and Propagation*, 63(4):1288–1300, 2015.

[8] G. Minatti, F. Caminita, E. Martini, M. Sabbadini, and S. Maci. Synthesis of modulated-metasurface antennas with amplitude, phase, and polarization control. *IEEE Transactions on Antennas and Propagation*, 64(9):3907–3919, 2016.

[9] D. R. Prado, A. Campa, M. Arrebola, M. R. Pino, J. A. Encinar, and F. Las-Heras. Design, manufacture, and measurement of a low-cost reflectarray for global earth coverage. *IEEE Antennas and Wireless Propagation Letters*, 15:1418–1421, 2016.

[10] D. R. Prado, M. Arrebola, M. R. Pino, R. Florencio, R. R. Boix, J. A. Encinar, and F. Las-Heras. Efficient crosspolar optimization of shaped-beam dual-polarized reflectarrays using full- wave analysis for the antenna element characterization. *IEEE Transactions on Antennas and Propagation*, 65(2):623–635, 2017.

[11] B. Imaz-Lueje, D. R. Prado, M. Arrebola, and M. R. Pino. Reflectarray antennas: A smart solution for new generation satellite mega-constellations in space communications. *Scientific Reports*, 10(1):1–13, 2020.

[12] A. Guarriello, D. Bresciani, H. Legay, G. Goussetis, and R. Loison. Design of circularly polarized and highly depointing reflectarrays with high polarization purity. In *2022 16th European Conference on Antennas and Propagation (EuCAP)*, pages 1–5, 2022.

[13] L. Moustafa, R. Gillard, F. Peris, R. Loison, H. Legay, and E. Girard. The phoenix cell: A new reflectarray cell with large bandwidth and rebirth capabilities. *IEEE Antennas and Wireless Propagation Letters*, 10:71–74, 2011.

[14] V. Richard, R. Gillard, R. Loison, H. Legay, M. Romier, J.-P. Martinaud, D. Bresciani, and F. Delepaux. Advanced synthesis of reflectarrays using a spherical mapping of the 2nd order phoenix cell. In *2019 13th European Conference on Antennas and Propagation (EuCAP)*, pages 1–5, 2019.

[15] D. Bresciani. A unified approach to the characterization of frequency and polarization selective surfaces. In *Proceedings of IEEE Antennas and Propagation Society International Symposium*, pages 1960–1963 vol.3, 1993.

[16] D. Bresciani, H. Legay, E. Labiole, and G. Caille. Antenne réseau réflecteur à compensation de polarisation croisée et procédé de réalisation d'une telle antenne. *Patent FR2957719*, 2011.